

# Practical representations of electromagnetic interferometry for GPR applications: a tutorial

Evert Slob\* and Kees Wapenaar

Department of Geotechnology, Delft University of Technology, Stevinweg 1, 2628 CN Delft, The Netherlands

Received November 2007, revision accepted March 2008

## ABSTRACT

Starting from the reciprocity theorems of the time-convolution and time-correlation types, several exact interferometric representations for electric and magnetic field Green's functions due to electric dipole and quadrupole sources are derived. The abundance of ambient noise, over a wide electromagnetic spectrum from sources in the atmosphere or in space, is used to define three different practical acquisition geometries that can be used to create new data from cross-correlations of the noise recordings. Similar setups are given for band limited transient sources to create new data from cross-correlations or cross-convolutions of the recordings from these transient sources. In all these applications the Earth can be arbitrarily anisotropic and dissipative as long as one receiver is located at the Earth's surface or in the air above. In applications where both receivers are located in the Earth we show that cross-correlations of such recordings lead to accurate new GPR data when the Earth is almost lossless.

## INTRODUCTION

The possibility of bringing the principle of daylight imaging, as we do with our eyes, over to other diffuse wavefields has been known for more than 20 years (Scherbaum 1987; Buckingham *et al.* 1992). Since the work of Weaver and Lobkis (Weaver and Lobkis 2001; Lobkis and Weaver 2001), many others have contributed to our understanding of Green's function retrieval from cross-correlating two recordings in a noise field. From one-dimensional and pulse-echo experiments the subject has evolved to arbitrary three-dimensional media, ranging from having statistical properties to being fully deterministic.

Many successful demonstrations of the method on ultrasonic, geophysical and oceanographic data as well as many theoretical developments have been published. Recent developments, in the branch of research that is based on reciprocity, are the extension for situations where time-reversal invariance does not hold (e.g., for electromagnetic waves in conducting media (Slob *et al.* 2006, 2007), acoustic waves in attenuating media (Snieder 2007) or general scalar diffusion phenomena (Snieder 2006)), as well as for situations where source-receiver reciprocity breaks down (e.g., in moving fluids (Wapenaar 2006; Godin 2006)). Recently a unified representation of Green's functions in terms of cross-correlations was developed that covers all these cases (Wapenaar *et al.* 2006; Snieder *et al.* 2007).

Another approach that has been developed is based on Green's functions representations in terms of cross-convolutions (Slob and Wapenaar 2007a,b). For an overview of the theory of

'seismic interferometry' or 'Green's function retrieval' and its applications to passive as well as controlled-source data, we refer to a reprint book, which contains a large number of papers on this subject (Wapenaar *et al.* 2008). Creating new data from measured data creates an enormous amount of possibilities to increase the data volume at little or no extra cost, thereby improving the imaging, inversion and characterization quality. This can be applied on actively recorded data, where only electric sources and electric and magnetic receivers are necessary to create data as if magnetic sources were used as well, thereby doubling the data volume.

Cross-borehole data can be generated from vertical radar profiles. Now that the regulators are decreasing the allowed output power of commercial ground-penetrating radar (GPR) systems it becomes more difficult in some areas to collect GPR data due to environmental noise. In such cases using this noise as a source for GPR data, the here described methods allow for reconstructing new GPR responses as if the noise were absent. One possible application is the so-called virtual multi-offset reflection profiling in cross-borehole GPR (Liu and He 2007).

The above possibilities also apply to passive or active noise data when cross-correlation methods are used. This is advantageous, e.g., in forensic applications, when it can be undesirable that others can find out that the measurements are collected. Passive methods have been known for a long time and they are often used for localization of electromagnetic fields (Knapp and Carter 1976) or for radiometry applications, e.g., for Earth observation (Ruf *et al.* 1988). The here presented method can be understood as a coherent form of radiometry and can be the tool to bridge the gap between the scales at which remote sensing oper-

---

\*e.c.slob@tudelft.nl

ates and the scale at which standard field GPR measurements are carried out. Also, for monitoring purposes it might be worthwhile to leave receivers in place and perform time lapse measurements by bringing the source to the field of interest when necessary or simply using the ambient noise.

In processing, imaging, inversion and characterization the accuracy of the information about the locations of the device is crucial and therefore the receiver locations must be known accurately, while the locations of the noise or transient sources are irrelevant as long as there are a sufficient number of them. In this tutorial paper we provide an overview of some general electromagnetic formulations and discuss several possible ground-penetrating radar applications of these recent developments.

### BASIC EQUATIONS AND RECIPROACITY

The time-domain Maxwell equations are most conveniently written down in a matrix-vector equation where the electric and magnetic medium parameters are time-convolution operators to allow for relaxation mechanisms. Mathematically all relaxation phenomena can be captured in the operator representing electric and magnetic conductivities, written in six-vector notation (Lindell *et al.* 1995) as:

$$\mathbf{D}_x \mathbf{u} + \mathbf{B} * \mathbf{u} + \mathbf{A} \partial_t \mathbf{u} = \mathbf{s}, \tag{1}$$

where it is assumed that the medium is at rest and that changes in the medium play a role on time scales much larger than the measurement scale. The vector  $\mathbf{u}(\mathbf{x}, t)$  contains the space- and time-dependent electric and magnetic field vectors, the source vector is denoted by  $\mathbf{s}(\mathbf{x}, t)$ , the position dependent matrix  $\mathbf{A}(\mathbf{x})$  contains the instantaneous parts of the electric permittivity and magnetic permeability and the position dependent and time-convolution operator  $\mathbf{B}(\mathbf{x}, t)$  takes all electric and magnetic time-relaxation phenomena into account;

$\mathbf{B}(\mathbf{x}, t) * \mathbf{u}(\mathbf{x}, t) = \int \mathbf{B}(\mathbf{x}, \tau) \mathbf{u}(\mathbf{x}, t - \tau) d\tau$ . The differential operator  $\mathbf{D}_x$  contains the spatial differential operator  $\partial_k$ ,  $k = 1, 2, 3$ , while  $\partial_t$  denotes differentiation with respect to the time coordinate  $t$ . The matrix-vector equation can be written out in full using the field and source vectors as:

$$\mathbf{u} = \begin{pmatrix} \mathbf{E} \\ \mathbf{H} \end{pmatrix}, \mathbf{s} = \begin{pmatrix} -\mathbf{J}^e \\ -\mathbf{J}^m \end{pmatrix}, \tag{2}$$

where the matrices are given by:

$$\mathbf{D}_x = \begin{pmatrix} \mathbf{O} & \mathbf{D}_0^T \\ \mathbf{D}_0 & \mathbf{O} \end{pmatrix}, \mathbf{D}_0 = \begin{pmatrix} 0 & -\partial_3 & \partial_2 \\ \partial_3 & 0 & -\partial_1 \\ -\partial_2 & \partial_1 & 0 \end{pmatrix},$$

$$\mathbf{A} = \begin{pmatrix} \boldsymbol{\varepsilon} & \mathbf{O} \\ \mathbf{O} & \boldsymbol{\mu} \end{pmatrix}, \mathbf{B} = \begin{pmatrix} \boldsymbol{\sigma}^e & \mathbf{O} \\ \mathbf{O} & \boldsymbol{\sigma}^m \end{pmatrix},$$

where the superscript  $T$  denotes the transpose of a vector or matrix, while  $\mathbf{O}$  is the  $3 \times 3$  null matrix and  $\boldsymbol{\varepsilon}(\mathbf{x})$ ,  $\boldsymbol{\mu}(\mathbf{x})$  denote the tensor components of the anisotropic electric permittivity and magnetic permeability of a heterogeneous medium. The tensor

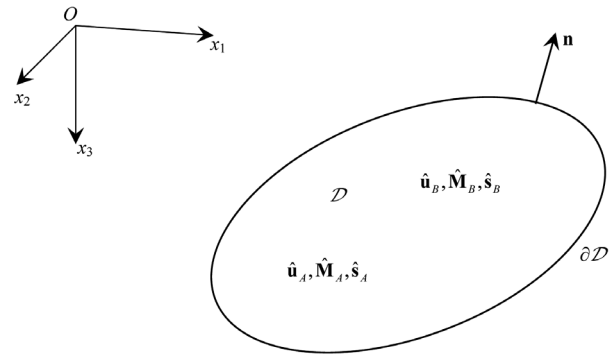


FIGURE 1 Configuration for the reciprocity theorems.

components of the anisotropic electric and magnetic conductivities of a heterogeneous medium are contained in  $\boldsymbol{\sigma}^e(\mathbf{x}, t)$ ,  $\boldsymbol{\sigma}^m(\mathbf{x}, t)$ , each component of which is a time convolution operator to allow for relaxation mechanisms.

The fact that the electric permittivity and magnetic permeability tensors are functions of space only, is not a restriction in the choice of models because all time-relaxation behaviour can be incorporated in the electric and magnetic conductivity tensors. Time convolutions are replaced by products through time-Fourier transformations and time differentiation is transformed to a multiplication with  $j\omega$ ,  $j$  being the imaginary unit and  $\omega$  the radial frequency. We define the time-Fourier transform of a space-time function  $\mathbf{f}(\mathbf{x}, t)$  as  $\hat{\mathbf{f}}(\mathbf{x}, \omega) = \int \mathbf{f}(\mathbf{x}, t) \exp(-j\omega t) dt$ . Applying the time-Fourier transformation to equation (1) yields:

$$\mathbf{D}_x \hat{\mathbf{u}} + \hat{\mathbf{B}} \hat{\mathbf{u}} + j\omega \mathbf{A} \hat{\mathbf{u}} = \hat{\mathbf{s}}. \tag{3}$$

We further define the unitary matrix,  $\mathbf{K}$  such that:

$$\mathbf{K} = \begin{pmatrix} -\mathbf{I} & \mathbf{O} \\ \mathbf{O} & \mathbf{I} \end{pmatrix}, \tag{4}$$

where  $\mathbf{I}$  in equation (4) denotes the unit  $3 \times 3$  matrix. In this paper the unit matrix  $\mathbf{I}$  is used as the  $3 \times 3$  and  $6 \times 6$  unit matrix without any confusion. Note that the matrix  $\mathbf{K}$  obeys the following symmetry relations,  $\mathbf{K} = \mathbf{K}^T = \mathbf{K}^{-1}$  which is often used in this paper. The matrix of partial differential operators obeys  $\mathbf{D}_x = \mathbf{D}_x^T = -\mathbf{K} \mathbf{D}_x \mathbf{K}$ , while for reciprocal media (de Hoop 1995), the matrices containing the medium parameters obey  $\mathbf{K} \mathbf{A} \mathbf{K} = \mathbf{A} = \mathbf{A}^T$  and  $\mathbf{K} \hat{\mathbf{B}} \mathbf{K} = \hat{\mathbf{B}} = \hat{\mathbf{B}}^T$ , which is a reasonable assumption for natural media.

In the next sections we derive general representations based on the reciprocity theorems of the time-convolution and time-correlation types. Reciprocity theorems interrelate two different states, labelled  $A$  and  $B$ , which can exist in a single domain, while the fields, sources and medium parameters can be completely different (Cheo 1965; de Hoop 1995). The medium parameters are arbitrary functions of space and the conductivities

are also a function of frequency and they occupy a certain domain  $\mathcal{D}$ , with closed boundary  $\partial\mathcal{D}$  and uniquely defined outward pointing unit normal vector  $\mathbf{n}$ , see Fig. 1.

We apply reciprocity to this bounded domain by using the local interaction quantity,  $\hat{\mathbf{u}}_A^T \mathbf{K} \mathbf{D}_x \hat{\mathbf{u}}_B - (\mathbf{D}_x \hat{\mathbf{u}}_A)^T \mathbf{K} \hat{\mathbf{u}}_B$ . Substitution of the basic equation (3) into this interaction quantity for both states leads to the local form of the reciprocity theorem:

$$\hat{\mathbf{u}}_A^T \mathbf{K} \mathbf{D}_x \hat{\mathbf{u}}_B - (\mathbf{D}_x \hat{\mathbf{u}}_A)^T \mathbf{K} \hat{\mathbf{u}}_B = \hat{\mathbf{u}}_A^T \mathbf{K} \hat{\mathbf{s}}_B - \hat{\mathbf{s}}_A^T \mathbf{K} \hat{\mathbf{u}}_B - \hat{\mathbf{u}}_A^T \mathbf{K} (j\omega \hat{\mathbf{M}}_B - j\omega \hat{\mathbf{M}}_A^T) \hat{\mathbf{u}}_B, \quad (5)$$

where the material matrices are given by,  $\hat{\mathbf{M}}_{A,B} = \mathbf{A} + \hat{\mathbf{B}}/(j\omega)$ . The material parameters in the block diagonal matrices  $\mathbf{A}_{A,B}$  and  $\hat{\mathbf{B}}_{A,B}$ , may show jump-discontinuities across certain boundaries inside  $\mathcal{D}$ . If we integrate over the domain,  $\mathcal{D}$  and apply Gauss' divergence theorem to the terms in the left-hand side of equation (5), containing the spatial derivative matrix, we must subdivide the domain into regions where the medium parameters vary continuously as a function of position. Then, integrating over these sub-domains leads to vanishing contributions from the internal boundaries due to the prevailing continuity conditions at those interfaces and the fact that only the continuous components are present in the terms on the left-hand side of equation (5). Only the surface integral remains over the closed outer boundary surface of the domain  $\mathcal{D}$ . We arrive at the frequency domain reciprocity relation of the time-convolution type:

$$\oint_{\partial\mathcal{D}} \hat{\mathbf{u}}_A^T \mathbf{K} \mathbf{N}_x \hat{\mathbf{u}}_B d^2\mathbf{x} = \int_{\mathcal{D}} (\hat{\mathbf{u}}_A^T \mathbf{K} \hat{\mathbf{s}}_B - \hat{\mathbf{s}}_A^T \mathbf{K} \hat{\mathbf{u}}_B) d^3\mathbf{x} - j\omega \int_{\mathcal{D}} \hat{\mathbf{u}}_A^T \mathbf{K} (\hat{\mathbf{M}}_B - \hat{\mathbf{M}}_A) \hat{\mathbf{u}}_B d^3\mathbf{x} \quad (6)$$

In this expression the matrix  $\mathbf{N}_x$  is arranged in the same way as the matrix  $\mathbf{D}_x$ , but with the derivatives replaced by the components of the unit normal vector and it obeys the same symmetry relations,  $\mathbf{N}_x = \mathbf{N}_x^T = -\mathbf{K} \mathbf{N}_x \mathbf{K}$ .

$$\mathbf{N}_x = \begin{pmatrix} \mathbf{O} & \mathbf{N}_0^T \\ \mathbf{N}_0 & \mathbf{O} \end{pmatrix}, \mathbf{N}_0 = \begin{pmatrix} 0 & -n_3 & n_2 \\ n_3 & 0 & -n_1 \\ -n_2 & n_1 & 0 \end{pmatrix}.$$

Equation (6) is a general theorem in the domain,  $\mathcal{D}$ , for reciprocal media, where the medium parameters can show finite jump as long as continuity conditions apply on the interfaces, across which these jumps occur. Notice that the volume integral vanishes when the medium parameters in the two states are the same.

Based on the reaction principle (Bojarski 1983), another starting point is the following interaction quantity,  $\hat{\mathbf{u}}_A^\dagger \mathbf{D}_x \hat{\mathbf{u}}_B - (\mathbf{D}_x \hat{\mathbf{u}}_A)^\dagger \hat{\mathbf{u}}_B$ , where the superscript  $\dagger$  denotes complex conjugation and transposition. Hence, the vector  $\hat{\mathbf{u}}_A^\dagger$ , represents a backward propagating wave if we work in a lossless medium, while it represents a backward propagating and damped wave or a backward diffusing electromagnetic field in a dissipative medium. This situation

with losses presents no problem, because  $\hat{\mathbf{u}}_A^\dagger$  represents the time reversed of a damped causal (wave)field and that is a completely anti-causal damped (wave)field in the direction of negative time. Hence it propagates and attenuates in the direction of negative time and this is how  $\hat{\mathbf{u}}_A^\dagger$  should be interpreted. Hence, the product of  $\hat{\mathbf{u}}_A^\dagger(\mathbf{x}, \omega)$  and  $\hat{\mathbf{u}}_B(\mathbf{x}, \omega)$  in the interaction quantity leads to the cross-correlation of two causal damped wavefields,  $\mathbf{u}_A(\mathbf{x}, t)$  and  $\mathbf{u}_B(\mathbf{x}, t)$ . That is why this interaction quantity leads to the local form of the reciprocity theorem of the time-correlation type. It is given by:

$$\hat{\mathbf{u}}_A^\dagger \mathbf{D}_x \hat{\mathbf{u}}_B + (\mathbf{D}_x \hat{\mathbf{u}}_A)^\dagger \hat{\mathbf{u}}_B = \hat{\mathbf{u}}_A^\dagger \hat{\mathbf{s}}_B + \hat{\mathbf{s}}_A^\dagger \hat{\mathbf{u}}_B - \hat{\mathbf{u}}_A^\dagger (j\omega \hat{\mathbf{M}}_B - j\omega \hat{\mathbf{M}}_A^\dagger) \hat{\mathbf{u}}_B, \quad (7)$$

where now the block diagonal matrix  $\hat{\mathbf{M}}_A^\dagger$  has changed to:

$$\hat{\mathbf{M}}_A^\dagger = \text{blockdiag} \left( \boldsymbol{\varepsilon}_A + j(\hat{\boldsymbol{\sigma}}_A^*)^* / \omega, \boldsymbol{\mu}_A + j(\hat{\boldsymbol{\sigma}}_A^*)^* / \omega \right), \quad (8)$$

and the superscript  $*$  denotes complex conjugation. It follows from equations (7) and (8) that the electric permittivity values in the two states are subtracted and the complex conjugate transpose of the conductivity tensor in state  $A$  is added to the conductivity tensor of state  $B$ . This occurs because of the earlier choice of putting all dispersion and dissipation mechanisms in the conductivity tensor. The real part of the conductivity tensor represents dissipation, while the imaginary part represents dispersion.

Again, we assume the medium parameters show no more than finite jump discontinuities and continuity conditions apply on the interfaces where these finite jumps occur. Then integrating equation (7) over the domain  $\mathcal{D}$  and applying the integral theorem of Gauss yields:

$$\oint_{\partial\mathcal{D}} \hat{\mathbf{u}}_A^\dagger \mathbf{N}_x \hat{\mathbf{u}}_B d^2\mathbf{x} = \int_{\mathcal{D}} (\hat{\mathbf{u}}_A^\dagger \hat{\mathbf{s}}_B + \hat{\mathbf{s}}_A^\dagger \hat{\mathbf{u}}_B) d^3\mathbf{x} - \int_{\mathcal{D}} \hat{\mathbf{u}}_A^\dagger (j\omega \hat{\mathbf{M}}_B - j\omega \hat{\mathbf{M}}_A^\dagger) \hat{\mathbf{u}}_B d^3\mathbf{x}. \quad (9)$$

Equation (9) is the general global correlation type reciprocity relation for self-adjoint media. Equations (6) and (9) are very useful as a starting point for deriving general representations for wavefield modelling and inversion and it is not restricted to electromagnetic wave phenomena, nor to internal interfaces satisfying continuity conditions (Wapenaar 2007). Here they are used in later sections to derive specific interferometric relations for the electromagnetic wavefield.

### The Green's matrix

The six-vectors  $\hat{\mathbf{u}}(\mathbf{x}, \omega)$  and  $\hat{\mathbf{s}}(\mathbf{x}, \omega)$  contain the electric and magnetic field vectors and the volume densities of electric and magnetic current sources. Of course, the field depends on the source type and its vector component. This dependence is specified through the definition of Green's functions, each one corresponding to a specific field type and component and generated by a particular source type and component. Consequently, there are six Green's functions for each source type and component and likewise, there are six Green's functions for each field type

and component. In total there are 36 electromagnetic Green's functions and these can be stored in a  $6 \times 6$  matrix. We start by rearranging the full source vector in a diagonal source matrix:

$$\mathbf{S} = (\mathbf{i}_1, \mathbf{i}_2, \mathbf{i}_3, \mathbf{i}_4, \mathbf{i}_5, \mathbf{i}_6) \delta(\mathbf{x} - \mathbf{x}^s) = \mathbf{I} \delta(\mathbf{x} - \mathbf{x}^s),$$

where each element of the source vector is taken as unity to define the Green's function, hence  $\mathbf{i}_m$  is the  $m^{\text{th}}$  column vector from the  $6 \times 6$  unit matrix  $\mathbf{I}$ , with the value '1' at the  $m^{\text{th}}$  location in an otherwise zero column vector. Similarly, we can associate a Green's vector that satisfies a modified basic equation:

$$\mathbf{D}_x \hat{\mathbf{g}}_m + \hat{\mathbf{B}} \hat{\mathbf{g}}_m + j\omega \mathbf{A} \hat{\mathbf{g}}_m = \mathbf{i}_m \delta(\mathbf{x} - \mathbf{x}^s), \tag{10}$$

where  $\hat{\mathbf{g}}_m(\mathbf{x}, \mathbf{x}^s, \omega)$  denotes the  $m^{\text{th}}$   $6 \times 1$  Green's field column vector at the observation point  $\mathbf{x}$  due to a point source of the  $m^{\text{th}}$  type at  $\mathbf{x}^s$ . If we take for example the electromagnetic field in an isotropic medium due to the vertical electric current source, we have the following matrix differential equation:

$$\begin{pmatrix} \eta & 0 & 0 & 0 & \partial_3 & -\partial_2 \\ 0 & \eta & 0 & -\partial_3 & 0 & \partial_1 \\ 0 & 0 & \eta & \partial_2 & -\partial_1 & 0 \\ 0 & -\partial_3 & \partial_2 & \zeta & 0 & 0 \\ \partial_3 & 0 & -\partial_1 & 0 & \zeta & 0 \\ -\partial_2 & \partial_1 & 0 & 0 & 0 & \zeta \end{pmatrix} \begin{pmatrix} \hat{G}_{13}^{EE} \\ \hat{G}_{23}^{EE} \\ \hat{G}_{33}^{EE} \\ \hat{G}_{13}^{ME} \\ \hat{G}_{23}^{ME} \\ \hat{G}_{33}^{ME} \end{pmatrix} = \begin{pmatrix} 0 \\ 0 \\ 0 \\ 0 \\ 0 \\ 0 \end{pmatrix} \delta(\mathbf{x} - \mathbf{x}^s), \tag{11}$$

with  $\eta = j\omega\epsilon + \sigma^e, \zeta = j\omega\mu + \sigma^m$  and the Green's elements  $\hat{G}_{kr}^{EE}, \hat{G}_{kr}^{ME}$  are indexed as follows; the first subscript refers to the field component and the second to the source component, while the first superscript refers to the recorded field type and the second to the source type. Hence, for the  $x_1$ -component of the magnetic current source, the matrix differential equation is written as:

$$\begin{pmatrix} \eta & 0 & 0 & 0 & \partial_3 & -\partial_2 \\ 0 & \eta & 0 & -\partial_3 & 0 & \partial_1 \\ 0 & 0 & \eta & \partial_2 & -\partial_1 & 0 \\ 0 & -\partial_3 & \partial_2 & \zeta & 0 & 0 \\ \partial_3 & 0 & -\partial_1 & 0 & \zeta & 0 \\ -\partial_2 & \partial_1 & 0 & 0 & 0 & \zeta \end{pmatrix} \begin{pmatrix} \hat{G}_{11}^{EM} \\ \hat{G}_{21}^{EM} \\ \hat{G}_{31}^{EM} \\ \hat{G}_{11}^{MM} \\ \hat{G}_{21}^{MM} \\ \hat{G}_{31}^{MM} \end{pmatrix} = \begin{pmatrix} 0 \\ 0 \\ 0 \\ 0 \\ 0 \\ 0 \end{pmatrix} \delta(\mathbf{x} - \mathbf{x}^s). \tag{12}$$

Note that equations (11) and (12) have the same operator matrix and we observe that the Green's vectors can be linearly combined to form:

$$(\hat{\mathbf{g}}_1, \hat{\mathbf{g}}_2, \hat{\mathbf{g}}_3, \hat{\mathbf{g}}_4, \hat{\mathbf{g}}_5, \hat{\mathbf{g}}_6)(\mathbf{x}, \mathbf{x}^s, \omega) = \hat{\mathbf{G}}(\mathbf{x}, \mathbf{x}^s, \omega),$$

where  $\hat{\mathbf{G}}(\mathbf{x}, \mathbf{x}^s, \omega)$  is the  $6 \times 6$  Green's field matrix. Together with the matrix representation for the Green's source matrix, we can

write the Green's matrix differential equation similar to equation (10) and combining for  $m = 1, 2, \dots, 6$ , as:

$$\mathbf{D}_x \hat{\mathbf{G}} + \hat{\mathbf{B}} \hat{\mathbf{G}} + j\omega \mathbf{A} \hat{\mathbf{G}} = \mathbf{I} \delta(\mathbf{x} - \mathbf{x}^s). \tag{13}$$

Since all combinations used here are linear in the fields and sources, we can apply the superposition principle to find solutions for the total field vector for arbitrary sources,  $\hat{\mathbf{s}}(\mathbf{x}, \omega)$ , of bounded support in space,  $\mathcal{D}_s$  and time, in terms of the here defined Green's function matrix as:

$$\hat{\mathbf{u}}(\mathbf{x}, \omega) = \int_{\mathcal{D}_s} \hat{\mathbf{G}}(\mathbf{x}, \mathbf{x}', \omega) \hat{\mathbf{s}}(\mathbf{x}', \omega) d^3 \mathbf{x}'. \tag{14}$$

Equation (14) implies that finding relations for the Green's matrix,  $\hat{\mathbf{G}}(\mathbf{x}, \mathbf{x}', \omega)$ , is sufficient to also find relations for the damped wave vector  $\hat{\mathbf{u}}(\mathbf{x}, \omega)$ .

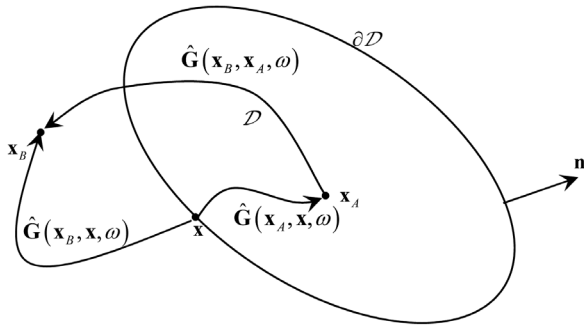
To arrive at a symmetry property of the Green's matrix, we use the same medium parameters in the two states,  $\mathbf{A}_B = \mathbf{A}_A = \mathbf{A}$  and  $\hat{\mathbf{B}}_B = \hat{\mathbf{B}}_A = \hat{\mathbf{B}}$ , both representing the actual state of a possible measurement. This eliminates the second integral in the right-hand side of equation (6). Then we assume that there is a ball  $\mathcal{B}$ , such that the domain  $\mathcal{D}$  fits completely inside  $\mathcal{B}$  and the medium outside  $\mathcal{B}$  is homogeneous and isotropic and we apply reciprocity to this ball  $\mathcal{B}$  instead of the domain  $\mathcal{D}$ . The radius of this ball is then taken to infinity and the Sommerfeld radiation conditions can be used to show that the boundary integral in equation (6) vanishes (Born and Wolf 1965). Then substitution of the definitions for the medium parameters and Green's and sources matrices in equation (6) yields the so-called source-receiver reciprocity relation:

$$\mathbf{K} \hat{\mathbf{G}}^T(\mathbf{x}_B, \mathbf{x}_A, \omega) \mathbf{K} = \hat{\mathbf{G}}(\mathbf{x}_A, \mathbf{x}_B, \omega), \tag{15}$$

which is written out in full for the indexed Green's sub matrices as:

$$\begin{pmatrix} \hat{G}_{kr}^{EE}(\mathbf{x}_B, \mathbf{x}_A, \omega) & -\hat{G}_{kp}^{ME}(\mathbf{x}_B, \mathbf{x}_A, \omega) \\ -\hat{G}_{jr}^{EM}(\mathbf{x}_B, \mathbf{x}_A, \omega) & \hat{G}_{jp}^{MM}(\mathbf{x}_B, \mathbf{x}_A, \omega) \end{pmatrix} = \begin{pmatrix} \hat{G}_{rk}^{EE}(\mathbf{x}_A, \mathbf{x}_B, \omega) & \hat{G}_{pk}^{EM}(\mathbf{x}_A, \mathbf{x}_B, \omega) \\ \hat{G}_{rj}^{ME}(\mathbf{x}_A, \mathbf{x}_B, \omega) & \hat{G}_{pj}^{MM}(\mathbf{x}_A, \mathbf{x}_B, \omega) \end{pmatrix}. \tag{16}$$

In equation (16) it can be seen that the electric field due to electric current sources is transposed upon interchanging source and receiver components and locations. This simply means that if one uses a particular antenna pair for a measurement, the outcome of the measurement is independent of the choice of which one to use as a transmitter or receiver. If the source and receiver positions are interchanged for electric fields due to magnetic sources, the Green's matrix is the negative transpose of the original Green's matrix, which means that also the source and receiver types have been interchanged. This means that if one uses a magnetic field


**FIGURE 2**

Configuration for interferometry by cross-convolution and cross-correlation.

antenna and an electric field antenna for a measurement and fixes their position and orientation, the outcome of the measurement differs only by its sign depending on the choice to use one as a transmitter and the other as a receiver.

### GREEN'S FUNCTION REPRESENTATIONS FOR INTERFEROMETRY BY CROSS-CONVOLUTION

To create new data from cross-convolving measured data, each measurement location represents a state in the reciprocity theorem. We do this by interchanging the original source and receiver locations and types using the source-receiver reciprocity relation of equation (15). Since the measurements at the two locations are taken simultaneously, the media in the two states are the same and equation (6) can be written in terms of the Green's matrix as:

$$\hat{\mathbf{G}}(\mathbf{x}_B, \mathbf{x}_A, \omega) [\chi_D(\mathbf{x}_A) - \chi_D(\mathbf{x}_B)] = \oint_{\partial D} \hat{\mathbf{G}}(\mathbf{x}_B, \mathbf{x}, \omega) \mathbf{N}_x \mathbf{K} \hat{\mathbf{G}}^T(\mathbf{x}_A, \mathbf{x}, \omega) \mathbf{K} d^2 \mathbf{x}, \quad (17)$$

where the characteristic function of the domain  $\mathcal{D}$  is given by:

$$\chi_D(\mathbf{x}) = \begin{cases} 0 & \text{for } \mathbf{x} \notin \mathcal{D} \cup \partial \mathcal{D} \\ \frac{1}{2} & \text{for } \mathbf{x} \in \partial \mathcal{D} \\ 1 & \text{for } \mathbf{x} \in \mathcal{D} \end{cases} \quad (18)$$

In case  $\mathbf{x}_A$  and  $\mathbf{x}_B$  are both located inside  $\mathcal{D}$ , on the boundary  $\partial \mathcal{D}$  or outside  $\mathcal{D} \cup \partial \mathcal{D}$  the boundary integral of equation (17) vanishes. In other situations, equation (17) is an exact representation of the Green's function between  $\mathbf{x}_A$  and  $\mathbf{x}_B$  in terms of products (equivalent to cross-convolutions in the time-domain) of recordings made at  $\mathbf{x}_A$  and  $\mathbf{x}_B$ , due to impulsive electric and magnetic point sources at  $\mathbf{x}$  along the boundary  $\partial \mathcal{D}$  and integrating over all these source locations. We take  $\mathbf{x}_A$  inside  $\mathcal{D}$  and  $\mathbf{x}_B$  outside  $\mathcal{D} \cup \partial \mathcal{D}$  so that we finally obtain:

$$\hat{\mathbf{G}}(\mathbf{x}_B, \mathbf{x}_A, \omega) = \oint_{\partial D} \hat{\mathbf{G}}(\mathbf{x}_B, \mathbf{x}, \omega) \mathbf{N}_x \mathbf{K} \hat{\mathbf{G}}^T(\mathbf{x}_A, \mathbf{x}, \omega) \mathbf{K} d^2 \mathbf{x} \quad (19)$$

and the corresponding configuration is depicted in Fig. 2.

In the present form equation (19) contains sources of both the electric and magnetic current types, which implies they should be available at all positions on the boundary. To prepare for practical applications we need to reformulate equation (19) such that it can be used with transient sources of a single type. The matrix  $\mathbf{N}_x$  must be diagonalized to obtain an expression that directly relates the right-hand side of equation (19) to cross-convolutions of specific components of measured field quantities. The first step in this process is to look at subsets of equation (6) and then we end up with a form that is similar to a subset of equation (19). We write the magnetic field vector that occurs in the boundary integral in terms of the electric field vector according to the index notation,  $\hat{H}_j(\mathbf{x}, \omega) = -(j\omega\mu)^{-1} \epsilon_{jmr} \partial_m \hat{E}_r(\mathbf{x}, \omega)$ , where  $\epsilon_{jmr} = -1$  for  $jmr = 132, 213, 321$ ,  $\epsilon_{jmr} = 1$  for  $jmr = 123, 231, 312$  and  $\epsilon_{jmr} = 0$  for other combinations of the subscripts.

Secondly, the material matrices do not occur in the reciprocity theorem because we have taken the two states the same and they vanish from equation (6). Hence, equation (6) can be written as:

$$\frac{1}{j\omega\mu} \oint_{\partial D} (\hat{E}_{r,A} n_m \partial_m \hat{E}_{r,B} - \hat{E}_{r,B} n_m \partial_m \hat{E}_{r,A}) d^2 \mathbf{x} = - \int_D (\hat{J}_{k,A}^e \hat{E}_{k,B} - \hat{J}_{r,B}^e \hat{E}_{r,A} + \hat{J}_{k,A}^m \hat{H}_{j,B} - \hat{J}_{p,B}^m \hat{H}_{p,A}) d^3 \mathbf{x}. \quad (20)$$

The details on how the reorganization of the left-hand side of equation (20) is established are given in Slob *et al.* (2007). Here it suffices to say that we have assumed that the medium in the neighbourhood of the boundary is homogeneous and isotropic. We now proceed to derive representations for the three independent Green's functions given in equation (16).

A general representation for any one of the Green's submatrices, as defined in the right-hand side of equation (16), can be written in a single equation as:

$$\hat{G}_{rk}^{F_B F_A}(\mathbf{x}_B, \mathbf{x}_A, \omega) = \frac{1}{j\omega\mu} \oint_{\partial D} \left\{ \hat{G}_{rp}^{F_B E}(\mathbf{x}_B, \mathbf{x}, \omega) n_m \partial_m \hat{G}_{kp}^{F_A E}(\mathbf{x}_A, \mathbf{x}, \omega) - \hat{G}_{kp}^{F_A E}(\mathbf{x}_A, \mathbf{x}, \omega) n_m \partial_m \hat{G}_{rp}^{F_B E}(\mathbf{x}_B, \mathbf{x}, \omega) \right\} d^2 \mathbf{x}, \quad (21)$$

where the superscripts  $F_A$ ,  $F_B$  stand for the fields strengths that must be recorded at  $\mathbf{x}_A$ ,  $\mathbf{x}_B$ , respectively. This implies that when  $F_A = E$  the electric field and when  $F_A = M$  the magnetic field must be recorded at  $\mathbf{x}_A$  and the same procedure is used for the receiver in  $\mathbf{x}_B$ . To arrive at equation (21) use has been made of equation (16) to replace  $\hat{G}_{kr}^{E F'}(\mathbf{x}, \mathbf{x}', \omega)$  with  $\pm \hat{G}_{rk}^{F' E}(\mathbf{x}', \mathbf{x}, \omega)$ , where the 'plus'-sign was chosen when  $F' = E$  and the 'minus'-sign when  $F' = M$ . The final result does not depend on it. Since the derivative is directed toward the unit normal vector of the boundary surface and acts on the points  $\mathbf{x}$ , it is interpreted as an electric quadrupole source directed along the unit normal. Equation (21) therefore represents the electric or magnetic field Green's function at  $\mathbf{x}_B$  due to an electric or magnetic dipole at  $\mathbf{x}_A$  as cross-convolutions of electric and/or magnetic field recordings due to impulsive electric dipole and quadrupole sources at  $\mathbf{x}$  on the boundary and integrated over the boundary.

TABLE 1  
Choices for the Green's states for the retrieval of the electric field Green's function due to an electric dipole source

	State A	State B
$\hat{J}_k^e(\mathbf{x}, \omega)$	$\delta_{kr} \delta(\mathbf{x} - \mathbf{x}_A)$	$\delta_{sp} \delta(\mathbf{x} - \mathbf{x}_B)$
$\hat{J}_k^m(\mathbf{x}, \omega)$	0	0
$\hat{E}_k(\mathbf{x}, \omega)$	$\hat{G}_{pk}^{EE}(\mathbf{x}, \mathbf{x}_A, \omega)$	$\hat{G}_{rs}^{EE}(\mathbf{x}, \mathbf{x}_B, \omega)$
$\hat{H}_j(\mathbf{x}, \omega)$	n.a.	n.a.
$\hat{\sigma}_{kr}^e(\mathbf{x}, \omega)$	$\hat{\sigma}_{pr}^e(\mathbf{x}, \omega)$	$\hat{\sigma}_{pr}^e(\mathbf{x}, \omega)$
$\chi_D(\mathbf{x})$	1	0

TABLE 2  
Choices for the Green's states for the retrieval of the magnetic field Green's function due to an electric dipole source

	State A	State B
$\hat{J}_k^e(\mathbf{x}, \omega)$	$\delta_{kr} \delta(\mathbf{x} - \mathbf{x}_A)$	0
$\hat{J}_k^m(\mathbf{x}, \omega)$	0	$\delta_{jp} \delta(\mathbf{x} - \mathbf{x}_B)$
$\hat{E}_k(\mathbf{x}, \omega)$	$\hat{G}_{pk}^{EE}(\mathbf{x}, \mathbf{x}_A, \omega)$	$\hat{G}_{rj}^{EM}(\mathbf{x}, \mathbf{x}_B, \omega)$
$\hat{H}_j(\mathbf{x}, \omega)$	$\hat{G}_{pk}^{ME}(\mathbf{x}, \mathbf{x}_A, \omega)$	n.a.
$\hat{\sigma}_{kr}^e(\mathbf{x}, \omega)$	$\hat{\sigma}_{pr}^e(\mathbf{x}, \omega)$	$\hat{\sigma}_{pr}^e(\mathbf{x}, \omega)$
$\chi_D(\mathbf{x})$	1	0

TABLE 3  
Choices for the Green's states for the retrieval of the electric field Green's function due to a magnetic dipole source

	State A	State B
$\hat{J}_k^e(\mathbf{x}, \omega)$	0	0
$\hat{J}_k^m(\mathbf{x}, \omega)$	$\delta_{jp} \delta(\mathbf{x} - \mathbf{x}_A)$	$\delta_{qs} \delta(\mathbf{x} - \mathbf{x}_B)$
$\hat{E}_k(\mathbf{x}, \omega)$	$\hat{G}_{kj}^{EM}(\mathbf{x}, \mathbf{x}_A, \omega)$	$\hat{G}_{rq}^{EM}(\mathbf{x}, \mathbf{x}_B, \omega)$
$\hat{H}_j(\mathbf{x}, \omega)$	$\hat{G}_{sj}^{MM}(\mathbf{x}, \mathbf{x}_A, \omega)$	$\hat{G}_{pq}^{MM}(\mathbf{x}, \mathbf{x}_B, \omega)$
$\hat{\sigma}_{kr}^e(\mathbf{x}, \omega)$	$\hat{\sigma}_{kr}^e(\mathbf{x}, \omega)$	$\hat{\sigma}_{kr}^e(\mathbf{x}, \omega)$
$\chi_D(\mathbf{x})$	1	0

When we make the choices for the two states specified in Table 1 the Green's function of the recorded electric field in  $\mathbf{x}_B$  due to an electric point source in  $\mathbf{x}_A$  is obtained from cross-correlations in the time domain of the electric field recordings in both  $\mathbf{x}_A$  and  $\mathbf{x}_B$  due to electric point sources on the boundary and summing over all these source contributions.

When we make the choices for the two states specified in Table 2 the Green's function of the recorded magnetic field in  $\mathbf{x}_B$  due to an electric point source in  $\mathbf{x}_A$  is obtained from cross-correlations in the time-domain of the electric field recordings in  $\mathbf{x}_A$  and magnetic field recordings in  $\mathbf{x}_B$  due to electric point sources on the boundary and summing over all these source contributions. When interchanging the field type recordings in  $\mathbf{x}_A$  and  $\mathbf{x}_B$

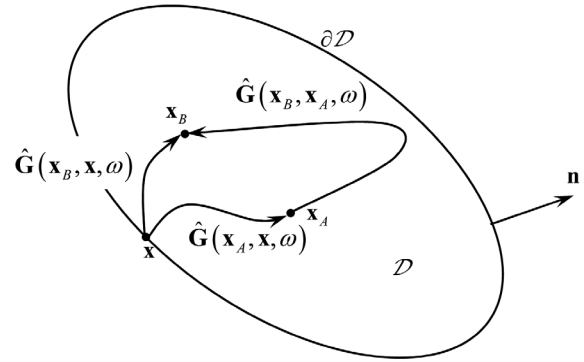


FIGURE 3  
Configuration for interferometry by cross-correlation.

the Green's function of the recorded electric field in  $\mathbf{x}_B$  due to a magnetic point source in  $\mathbf{x}_A$  is obtained.

Finally, when we make the choices for the two states specified in Table 3 the Green's function of the recorded magnetic field in  $\mathbf{x}_B$  due to a magnetic point source in  $\mathbf{x}_A$  is obtained from cross-correlations in the time-domain of the magnetic field recordings in both  $\mathbf{x}_A$  and  $\mathbf{x}_B$  due to electric point sources on the boundary and summing over all these source contributions.

### GREEN'S FUNCTION REPRESENTATIONS FOR INTERFEROMETRY BY CROSS-CORRELATION

As was done for representations of interferometry by cross-correlation, here similar expressions are given for interferometry by cross-correlation. Again, the media are taken the same in the two states and we substitute previous choices for the Green's function and sources matrices and use equation (15) to interchange the original sources and receivers in equation (9) to arrive at:

$$\hat{G}(\mathbf{x}_B, \mathbf{x}_A, \omega) \chi_D(\mathbf{x}_A) + \hat{G}^\dagger(\mathbf{x}_A, \mathbf{x}_B, \omega) \chi_D(\mathbf{x}_B) - \oint_{\partial D} \hat{G}(\mathbf{x}_B, \mathbf{x}, \omega) \mathbf{N}_x \hat{G}^\dagger(\mathbf{x}_A, \mathbf{x}, \omega) d^2 \mathbf{x} + 2 \int_D \hat{G}(\mathbf{x}_B, \mathbf{x}, \omega) \Re(\hat{\mathbf{B}}) \hat{G}^\dagger(\mathbf{x}_A, \mathbf{x}, \omega) d^3 \mathbf{x} \quad (22)$$

where the real part of the conductivity matrix is denoted by  $\Re(\hat{\mathbf{B}})$  and is given by  $\Re(\hat{\mathbf{B}}) = \text{blockdiag}(\Re(\hat{\sigma}^e), \Re(\hat{\sigma}^m))$ . Equation (22) is the general exact representation of the electromagnetic Green's function between  $\mathbf{x}_A$  and  $\mathbf{x}_B$  in terms of products of Green's matrices representing point source responses at  $\mathbf{x}_B$  and complex conjugate transposed Green's matrices representing point source responses at  $\mathbf{x}_A$  (equivalent to cross-correlations in the time-domain of recordings made at  $\mathbf{x}_A$  and  $\mathbf{x}_B$ ), due to impulsive electric and magnetic point sources at  $\mathbf{x}$  along the boundary  $\partial D$  and integrating over all these source locations. First it is observed that the presence of the dissipation term in the volume integral on the right-hand side of equation (22) is only over the domain of reciprocity, implying that outside this domain the medium can be dissipative without any change in the representation. A second

observation is that the left-hand side of equation (22) vanishes only when both  $\mathbf{x}_A$  and  $\mathbf{x}_B$  are taken outside the domain and its boundary. This means that the configuration of Figs 2 and 3 are suitable for this type of interferometry.

In the present form equation (22) contains sources of both the electric and magnetic current types, which implies they should be available at all positions on the boundary. To prepare for practical applications we need to reformulate equation (22) such that it can be used with transient or uncorrelated noise sources of a single type. The matrix  $\mathbf{N}_x$  must be diagonalized to obtain an expression that directly relates the right-hand side of equation (22) to cross-correlations of specific components of measured field quantities. The first step is the same as was used to arrive at equation (20) from equation (6). We write the magnetic field vector that occurs in the boundary integral in terms of the electric field vector. Secondly, in all our applications, we will assume natural material that presents no dissipation in its magnetic properties and hence we take  $\hat{\boldsymbol{\sigma}}^m(\mathbf{x}, \omega) = \mathbf{O}$ . Then equation (9) can be written as:

$$\begin{aligned} & \frac{1}{j\omega\mu} \oint_{\partial\mathcal{D}} \left( \hat{E}_{r,A}^* n_m \partial_m \hat{E}_{r,B} - \hat{E}_{r,B} n_m \partial_m \hat{E}_{r,A}^* \right) d^2\mathbf{x} = \\ & 2 \int_{\mathcal{D}} \hat{E}_{k,B} \Re \left( \hat{\sigma}_{kr}^e \right) \hat{E}_{r,A}^* d^3\mathbf{x} \\ & + \int_{\mathcal{D}} \left\{ \left( \hat{J}_{k,A}^e \right)^* \hat{E}_{k,B} + \hat{J}_{r,B}^e \hat{E}_{r,A}^* + \left( \hat{J}_{j,A}^m \right)^* \hat{H}_{j,B} + \hat{J}_{p,B}^m \hat{H}_{p,A}^* \right\} d^3\mathbf{x}. \end{aligned} \quad (23)$$

We now proceed to derive representations from equation (23) for the three independent Green's functions given in equation (16) in terms of cross-correlations of observed electromagnetic wavefields.

A general representation for any one of the Green's sub-matrices can be written in a single equation as:

$$\begin{aligned} & \hat{G}_{rk}^{F_A F_B}(\mathbf{x}_B, \mathbf{x}_A, \omega) \chi_{\mathcal{D}}(\mathbf{x}_A) \pm \left\{ \hat{G}_{rk}^{F_A F_B}(\mathbf{x}_B, \mathbf{x}_A, \omega) \right\}^* \chi_{\mathcal{D}}(\mathbf{x}_B) \\ & = -2 \int_{\mathcal{D}} \hat{G}_{rp}^{F_B E}(\mathbf{x}_B, \mathbf{x}, \omega) \Re \left\{ \hat{\sigma}_{pq}^e(\mathbf{x}, \omega) \right\} \left\{ \hat{G}_{qk}^{F_A E}(\mathbf{x}_A, \mathbf{x}, \omega) \right\}^* d^3\mathbf{x} - \frac{1}{j\omega\mu} \\ & \times \oint_{\partial\mathcal{D}} \left[ \hat{G}_{rj}^{F_B E}(\mathbf{x}_B, \mathbf{x}, \omega) \left\{ n_n \partial_n \hat{G}_{kj}^{F_A E}(\mathbf{x}_A, \mathbf{x}, \omega) \right\}^* \right. \\ & \left. - \left\{ \hat{G}_{kp}^{F_A E}(\mathbf{x}_A, \mathbf{x}, \omega) \right\}^* n_m \partial_m \hat{G}_{rp}^{F_B E}(\mathbf{x}_B, \mathbf{x}, \omega) \right] d^2\mathbf{x}, \end{aligned} \quad (24)$$

where in the left-hand side the 'plus'-sign must be taken when  $F_A = F_B$  and the 'minus'-sign must be taken when  $F_A \neq F_B$ . Equation (24) represents the electric or magnetic field Green's function at  $\mathbf{x}_B$  due to an electric or magnetic dipole source at  $\mathbf{x}_A$  as integrated contributions from electric and/or magnetic recordings due to two different types of sources. The first integral on the right-hand side represents the frequency domain expression of a contribution from cross-correlations in the time-domain of recorded fields due to electric dipole sources, each with the strength of the local real parts of the conductivity at  $\mathbf{x}$  in  $\mathcal{D}$  and then integrated over the whole domain  $\mathcal{D}$ . The second integral on the right-hand side represents the frequency domain expression of a contribution from cross-correlations in the time-domain of

field recordings due to impulsive electric dipoles and quadrupoles at  $\mathbf{x}$  on the boundary and integrated over the boundary.

The volume integral in the right-hand side of equation (24) accounts for the energy lost over the paths that are not part of the physical paths between  $\mathbf{x}_A$  and  $\mathbf{x}_B$ . When the medium is dissipative everywhere, the boundary can be taken to infinity resulting in a vanishing contribution. Then the Green's function can be directly retrieved from these volume sources only (Snieder 2006). When the dissipation is weak, the volume integral can be neglected and a discussion about this aspect is given in Slob *et al.* (2007).

When we make the choices for the two states specified in Table 1, the Green's function of the recorded electric field in  $\mathbf{x}_B$  due to an electric point source in  $\mathbf{x}_A$  is obtained from cross-correlations in the time-domain of the electric field recordings in both  $\mathbf{x}_A$  and  $\mathbf{x}_B$  due to electric point sources on the boundary and summing over all these source contributions.

When we make the choices for the two states specified in Table 2, the Green's function of the recorded magnetic field in  $\mathbf{x}_B$  due to an electric point source in  $\mathbf{x}_A$  is obtained from cross-correlations in the time-domain of the electric field recordings in  $\mathbf{x}_A$  and magnetic field recordings in  $\mathbf{x}_B$  due to electric point sources on the boundary and summing over all these source contributions. When interchanging the field type recordings in  $\mathbf{x}_A$  and  $\mathbf{x}_B$  the Green's function of the recorded electric field in  $\mathbf{x}_B$  due to a magnetic point source in  $\mathbf{x}_A$  is obtained.

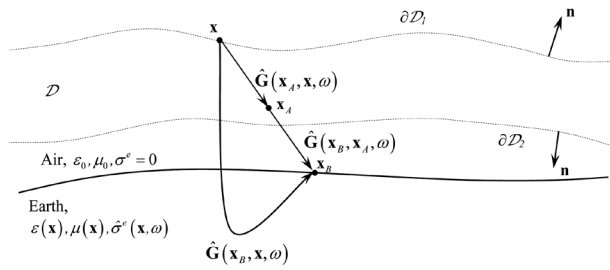
Finally, when we make the choices for the two states specified in Table 3, the Green's function of the recorded magnetic field in  $\mathbf{x}_B$  due to a magnetic point source in  $\mathbf{x}_A$  is obtained from cross-correlations in the time-domain of the magnetic field recordings in both  $\mathbf{x}_A$  and  $\mathbf{x}_B$  due to electric point sources on the boundary and summing over all these source contributions.

## APPLICATIONS: SOURCES IN OR ABOVE THE ATMOSPHERE

The applications we discuss here are with sources in or above the atmosphere. There is a lot of electromagnetic energy radiated toward the Earth from different kinds of sources in space and the sun is a well-known example of it. The ionosphere is open for sufficiently wide bands such that passive GPR applications should be possible.

We can exploit this presence of far away sources by creating a domain with the horizontal sides extending to 'infinity', while the top side of the domain can be placed anywhere above the highest receiver location and the bottom side of the domain is located just above the Earth's surface, see Fig. 4. This puts the heterogeneous and dissipative Earth outside the whole domain and the energy dissipation in the Earth presents no problem in the Green's function retrieval by cross-correlation.

From previous studies we know that the important contributions come from the source points that are stationary for physical paths between the receiver locations  $\mathbf{x}_A$  and  $\mathbf{x}_B$  (Schuster 2001, 2004). The path depicted in Fig. 4 is stationary for the


**FIGURE 4**

Configuration for the practical situation of sources in or above the Earth's atmosphere for Green's function retrieval by cross-correlation, where the Earth is outside.

direct waves between the receivers at  $\mathbf{x}_A$  and  $\mathbf{x}_B$  but not necessarily for other paths, which demonstrates that not all points on the boundary are of equal importance. It has been shown in Slob and Wapenaar (2007) that for the cross-correlation of recorded fields, contributions from the boundary  $\partial D_2$  in Fig. 4 lead to non-physical events that all cancel each other and all physical contributions come from the boundary  $\partial D_1$ . Absence of sources on  $\partial D_2$  does not lead to any problems in Green's functions retrieval. The reason is that non-physical events that arise from sources on  $\partial D_1$  and that would be cancelled by the same non-physical events arising with opposite sign from sources on  $\partial D_2$ , arrive at negative times, or at least before the first physical arrival. Hence, the presence of these non-physical events, which remain in the data in absence of sources on  $\partial D_2$ , are easily identified. Now, in equation (24) still quadrupole contributions are present for which an approximation must be found. We assume that the boundary is so far away from the receivers that Fraunhofer conditions apply for sources on the boundary  $\partial D_1$ . Because all waves that are generated at  $\partial D_1$  that travel initially downward are recorded at  $\mathbf{x}_A$  and  $\mathbf{x}_B$ , while the waves that travel initially upward never return in absence of any heterogeneity above the boundary  $\partial D_1$ . In that case the quadrupole contributions from sources at  $\partial D_1$  can be approximated as:

$$n_m \partial_m \mathbf{G}(\mathbf{x}', \mathbf{x}, \omega) \approx -\frac{j\omega}{c} \mathbf{G}(\mathbf{x}', \mathbf{x}, \omega), \quad (25)$$

where the sign corresponds to the inward travelling waves (Wapenaar *et al.* 2005) and are taken because these are recorded. When the domain  $\mathcal{D}$  is lossless, only the boundary integral over  $\partial D_1$  remains,  $\mathbf{x}_A$  is inside  $\mathcal{D}$  and  $\mathbf{x}_B$  is outside  $\mathcal{D}$  and with the aid of equation (25), equation (24) reduces to:

$$\hat{G}_{rk}^{F_B F_A}(\mathbf{x}_B, \mathbf{x}_A, \omega) \approx -\frac{2}{\mu c} \int_{\partial D_1} \hat{G}_{rj}^{F_B E}(\mathbf{x}_B, \mathbf{x}, \omega) \left\{ \hat{G}_{kj}^{F_A E}(\mathbf{x}_A, \mathbf{x}, \omega) \right\}^* d^2 \mathbf{x}. \quad (26)$$

Equation (26) demonstrates that measuring all components of the electric and/or magnetic fields due to electric dipole sources suffices to retrieve, by cross-correlation, all components of the electric and magnetic fields due to all components of electric and magnetic dipole sources.

### Uncorrelated noise sources

Assume the sources on the boundary are spatially uncorrelated noise sources with spectra  $\hat{N}_s(\mathbf{x}, \omega)$ , satisfying:

$$\left\langle \hat{N}_s^*(\mathbf{x}, \omega) \hat{N}_q(\mathbf{x}', \omega) \right\rangle = \frac{2}{\mu c} \delta_{sq} \delta(\mathbf{x} - \mathbf{x}') \hat{S}(\omega), \quad (27)$$

where  $\hat{S}(\omega)$  is the noise power spectrum. The recorded electric fields due to these sources can be written as:

$$\begin{aligned} \hat{F}_{A:k}^{\text{obs}}(\mathbf{x}_A, \omega) &= \int_{\mathbf{x} \in \partial D_1} \hat{G}_{ks}^{F_A E}(\mathbf{x}_A, \mathbf{x}, \omega) \hat{N}_s(\mathbf{x}, \omega) d^2 \mathbf{x} \\ \hat{F}_{B:r}^{\text{obs}}(\mathbf{x}_B, \omega) &= \int_{\mathbf{x}' \in \partial D_1} \hat{G}_{rj}^{F_B E}(\mathbf{x}_B, \mathbf{x}', \omega) \hat{N}_j(\mathbf{x}', \omega) d^2 \mathbf{x}', \end{aligned} \quad (28)$$

where the observed field  $\hat{F}_A = \hat{E}$  when the superscript in the right-hand side  $F_A = E$  and  $\hat{F}_A = \hat{H}$  when the superscript  $F_A = H$ . Using equations (27) and (28) we see that the cross-correlation of the observed electric and/or magnetic fields is given by:

$$\left\langle \hat{F}_{B:r}^{\text{obs}}(\mathbf{x}_B, \omega) \hat{F}_{A:k}^{\text{obs}}(\mathbf{x}_A, \omega) \right\rangle = \frac{2}{\mu c} \int_{\partial D_1} \hat{G}_{rs}^{F_B E}(\mathbf{x}_B, \mathbf{x}, \omega) \left\{ \hat{G}_{ks}^{F_A E}(\mathbf{x}_A, \mathbf{x}, \omega) \right\}^* d^2 \mathbf{x} \hat{S}(\omega), \quad (29)$$

which substituted in equation (26) leads to:

$$\hat{G}_{rk}^{F_B F_A}(\mathbf{x}_B, \mathbf{x}_A, \omega) \hat{S}(\omega) \approx -\left\langle \hat{F}_{B:r}^{\text{obs}}(\mathbf{x}_B, \omega) \hat{F}_{A:k}^{\text{obs}}(\mathbf{x}_A, \omega) \right\rangle, \quad (30)$$

which is the desired expression showing that the cross-correlation of electric and or magnetic field measurements simultaneously obtained at two locations  $\mathbf{x}_A$  and  $\mathbf{x}_B$  yields the Green's function between these two points. In the time domain, equation (30) can be written as:

$$\int_{t'=-\infty}^{\infty} G_{rk}^{F_B F_A}(\mathbf{x}_B, \mathbf{x}_A, t') S(t-t') dt' \approx -\left\langle \int_{t'=-\infty}^{\infty} F_{B:r}(\mathbf{x}_B, t+t') F_{A:k}^*(\mathbf{x}_A, t') dt' \right\rangle. \quad (31)$$

Notice that the choice of spatially uncorrelated noise sources implies that no separate source contributions need to be recorded and all sources can be active at the same time. In case the noise sources suffer from some spatial correlation, undesired events can be generated, which possibly introduce some artefacts. This depends on the degree of correlation between the sources and when the spatial correlation between the noise sources becomes too large all sources should be transients. Then for each source a separate recording can be made. This allows first cross-correlating the recordings and then summing over all sources.

### Transient sources

When uncorrelated noise sources do not exist on the boundary, equation (26) can be used with controlled or uncontrolled transient sources, with the restriction that these sources must be active in separate time windows allowing for independent measurements for each source. Let the source in the frequency domain be represented by  $\hat{s}^j(\mathbf{x}, \omega)$  for a source in the  $x_j$ -direction at position  $\mathbf{x}$ , which can be different for each direction and for each

source position. The power spectrum of the sources is defined as:

$$\hat{S}^j(\mathbf{x}, \omega) = \hat{s}^j(\mathbf{x}, \omega) \left\{ \hat{s}^j(\mathbf{x}, \omega) \right\}^* \quad (32)$$

The field observed at the two stations can be written as:

$$\hat{F}_{k,s}^{\text{obs}}(\mathbf{x}_{A,B}, \mathbf{x}, \omega) = \hat{G}_{ks}^{F_{A,B}E}(\mathbf{x}_{A,B}, \mathbf{x}, \omega) \hat{s}^s(\mathbf{x}, \omega). \quad (33)$$

Substitution of equation (33) and using equation (32) in equation (26) results in:

$$\hat{G}_{rk}^{F_B F_A}(\mathbf{x}_B, \mathbf{x}_A, \omega) \hat{S}_0(\omega) = \int_{\partial \mathcal{D}_1} \hat{Q}^j(\mathbf{x}, \omega) \hat{F}_{B,r,j}^{\text{obs}}(\mathbf{x}_B, \mathbf{x}, \omega) \left\{ \hat{F}_{A,k,j}^{\text{obs}}(\mathbf{x}_A, \mathbf{x}, \omega) \right\}^* d^2 \mathbf{x}. \quad (34)$$

The factor  $\hat{S}_0(\omega)$  in the left-hand side of equation (34) is an arbitrarily chosen desired power spectrum of the source, while the factor  $\hat{Q}^j(\mathbf{x}, \omega)$  in the right-hand side is a shaping factor given by:

$$\hat{Q}^j(\mathbf{x}, \omega) = -2 \frac{Y \hat{S}_0(\omega)}{\hat{S}^j(\mathbf{x}, \omega)}, \quad (35)$$

with  $Y$  being the plane wave admittance given by  $Y = 1/(\mu c)$ . The presence of the shaping filter implies that these source signatures should be known. In this way a correlation result can be obtained for each separate source position and correlation gathers can be constructed, which can allow for the identification of spurious events that possibly occur due to the assumption that Fraunhofer conditions apply to the geometry.

### Green's function retrieval by cross-convolution

When transient sources are available, cross-convolution techniques can be used. We use the same configuration depicted in Fig. 4 but now the boundary  $\partial \mathcal{D}_1$  gives a vanishing contribution (see Slob and Wapenaar 2007) and all physical events come from  $\partial \mathcal{D}_2$  as is depicted in Fig. 5. The non-physical events that are generated cancel each other when the quadrupole contribution is correctly taken into account.

We assume again that Fraunhofer conditions apply to approx-

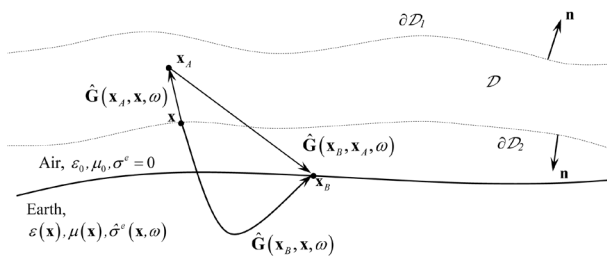


**FIGURE 5**

Configuration for the practical situation of sources in or above the Earth's atmosphere for Green's function retrieval by cross-convolution, where the Earth is outside  $\mathcal{D}$ .

imate the quadrupole term. One must again choose a direction of the wavefield leaving the boundary surface. For the point  $\mathbf{x}_B$  being outside of  $\mathcal{D}$ , the waves leaving the boundary in the outward direction are recorded, while the waves leaving the domain in the inward direction never return. In cross-convolution methods the traveltimes from the sources on the boundary to the two receiver locations are added. Consequently for the point  $\mathbf{x}_A$  being inside of  $\mathcal{D}$ , the waves that travel direct from the boundary to  $\mathbf{x}_A$  lead to physical events when cross-convolved in the time-domain with the recording made at  $\mathbf{x}_B$ . Hence we approximate the quadrupole term now for point  $\mathbf{x}_A$  as defined in equation (25) and for  $\mathbf{x}_B$  as:

$$n_m \partial_m \mathbf{G}(\mathbf{x}_B, \mathbf{x}, \omega) \approx \frac{j\omega}{c} \mathbf{G}(\mathbf{x}_B, \mathbf{x}, \omega). \quad (36)$$

Substitution of these approximations in equation (21) yields:

$$\hat{G}_{rk}^{F_B F_A}(\mathbf{x}_B, \mathbf{x}_A, \omega) \approx -\frac{2}{\mu c} \oint_{\partial \mathcal{D}} \hat{G}_{rp}^{F_B E}(\mathbf{x}_B, \mathbf{x}, \omega) \hat{G}_{kp}^{F_A E}(\mathbf{x}_A, \mathbf{x}, \omega) d^2 \mathbf{x}. \quad (37)$$

In the cross-convolution method the dissipative character of the medium inside or outside the domain  $\mathcal{D}$  is irrelevant for the results and hence we can imagine that the boundary  $\partial \mathcal{D}_1$  would be somewhere in the Earth below the surface. Then  $\mathbf{x}_A$  moves from the inside to the outside of  $\mathcal{D}$ , while for  $\mathbf{x}_B$  the opposite occurs, both unit normal vectors reverse their direction and now  $\chi_B(\mathbf{x}) = 1$ , while  $\chi_A(\mathbf{x}) = 0$ , so that the total result remains unchanged, as expected. An expression similar to equation (34) can be derived but now with cross-convolutions in the time-domain instead of cross-correlations:

$$\hat{G}_{rk}^{F_B F_A}(\mathbf{x}_B, \mathbf{x}_A, \omega) \hat{S}_0(\omega) = \int_{\partial \mathcal{D}_1} \hat{Q}^j(\mathbf{x}, \omega) \hat{F}_{B,r,j}^{\text{obs}}(\mathbf{x}_B, \mathbf{x}, \omega) \hat{F}_{A,k,j}^{\text{obs}}(\mathbf{x}_A, \mathbf{x}, \omega) d^2 \mathbf{x}. \quad (38)$$

In this equation the desired power spectrum  $\hat{S}_0(\omega)$  and the shaping factor  $\hat{Q}^j(\mathbf{x}, \omega)$  are the same as defined above.

### Both observation points at or below the Earth's surface

In situations where we would like to have our receivers both at or below the surface and use air or space born sources, either noise or transient sources, we need to incorporate the Earth and both observation points in the domain  $\mathcal{D}$  and as a consequence only cross-correlation methods can be applied. In this case the dissipative terms show up in the expressions for the Green's function retrieval and we must assume that the losses are weak or absent.

Secondly, sources on the closed boundary are necessary in principle. If only sources on a part of the boundary are available, non-physical events can remain in the data because of incomplete destructive interference in the cross-correlation process. Wapenaar (2006) showed that when the heterogeneities inside the Earth are so strong that the wavefield becomes diffuse, these non-physical events become strongly suppressed and contributions from a boundary deep in the Earth is not necessary because

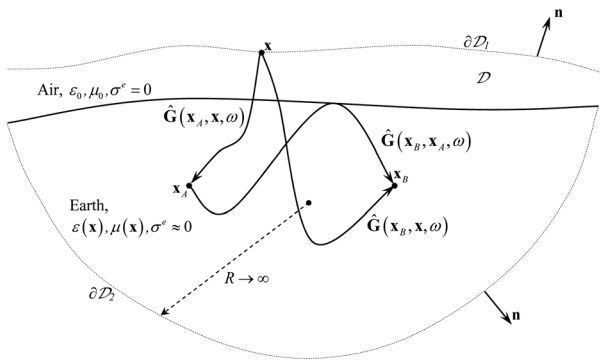


**FIGURE 6**  
Configuration for the practical situation of sources in or above the Earth's atmosphere for Green's function retrieval by cross-correlation, where the Earth is inside  $\mathcal{D}$ .

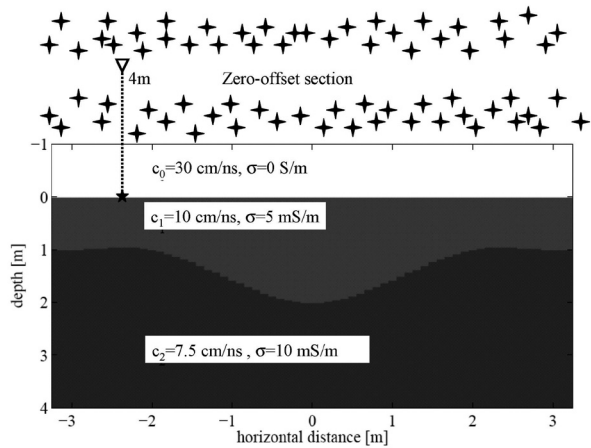


**FIGURE 7**  
A simple syncline model with non-zero conductivity values in the two subsurface layers. The configuration is used for the 2D TE-mode numerical examples of retrieving the Green's function between two vertically spaced receivers, from cross-convolutions and cross-correlations of recordings at these two receivers, due to sources in the air.

the heterogeneous Earth acts as a complicated mirror, bringing all energy up to the surface after many multiple interactions. This leads to the possibility to retrieve the Green's function to a high degree of accuracy from one-sided illumination. The configuration is depicted in Fig. 6 for the situation with both receivers inside the Earth. The receivers can be freely placed anywhere inside the boundary from the connection of  $\partial\mathcal{D}_1$  and  $\partial\mathcal{D}_2$ .

Taking into account that both  $\mathbf{x}_A$  and  $\mathbf{x}_B$  are in  $\mathcal{D}$ , equation (24) reduces, with the substitution of the approximation given in equation (25) to:

$$2\Re\left\{\hat{G}_{rk}^{F_A F_B}(\mathbf{x}_B, \mathbf{x}_A, \omega)\right\} \approx -\frac{2}{\mu c} \int_{\partial\mathcal{D}_1} \hat{G}_{rj}^{F_B E}(\mathbf{x}_B, \mathbf{x}, \omega) \left\{\hat{G}_{kj}^{F_A E}(\mathbf{x}_A, \mathbf{x}, \omega)\right\}^* d^2\mathbf{x}, \quad (39)$$

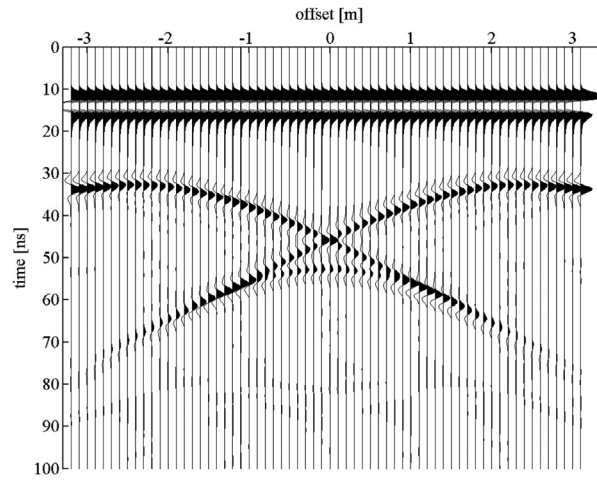


**FIGURE 8**  
The direct modelled zero horizontal offset result of the 2D TE-mode electric field measured at the Earth's surface due to an elevated source.

when both  $F_A$  and  $F_B$  are the same. Repeating this procedure when  $F_A$  and  $F_B$  are different gives the expression for the magnetic field Green's functions due to electric dipoles, or *vice versa*:

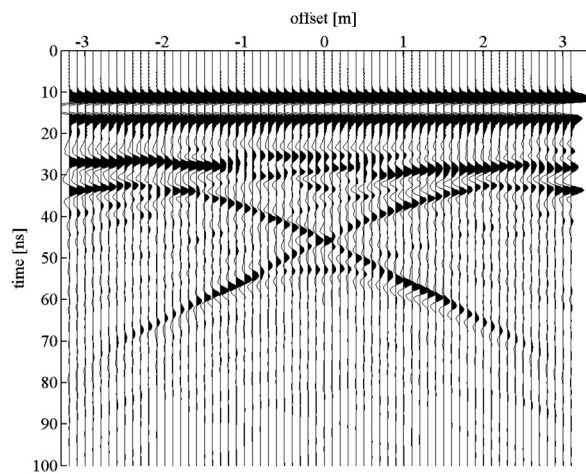
$$2i\Im\left\{\hat{G}_{rk}^{F_A F_B}(\mathbf{x}_B, \mathbf{x}_A, \omega)\right\} \approx -\frac{2}{\mu c} \int_{\partial\mathcal{D}_1} \hat{G}_{rj}^{F_B E}(\mathbf{x}_B, \mathbf{x}, \omega) \left\{\hat{G}_{kj}^{F_A E}(\mathbf{x}_A, \mathbf{x}, \omega)\right\}^* d^2\mathbf{x}, \quad (40)$$

Equations (39) and (40) show that either the real or imaginary part of the Green's function is retrieved. This is sufficient because each Green's function is a causal time-function, meaning it is fully determined by either its real or imaginary part in the frequency domain. The real and imaginary parts of such functions form a Hilbert transform pair. Extensions of these relations to account for band limited signals, either uncorrelated noise or transient source signals, are easily found using the definitions of equations (27)–(29) for noise sources and the definitions of equations (32), (33) and (45) for transient sources.

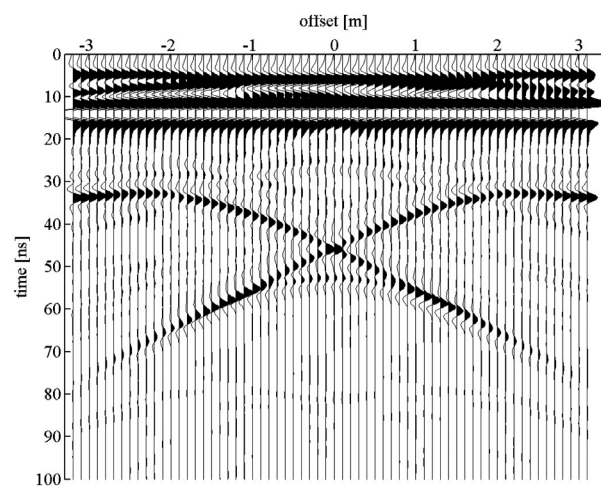
### NUMERICAL EXAMPLES

To give an illustration of the possibilities we show some 2D TE-mode numerical examples with correlation and convolution methods. The model consists of a simple syncline structure below the Earth's surface and we assume the sources to be distributed at two distinct non-overlapping height intervals above the surface. The two subsurface layers show a decreasing velocity and increasing conductivity with depth, see Fig. 7. The two points that are used to record the model response due to sources in the upper half space have zero horizontal offset and a 4 m vertical offset.

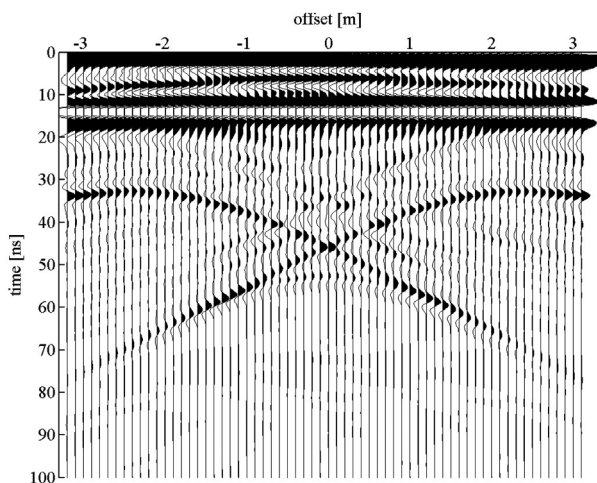
Figure 8 shows the direct modelled result of the recorded electric field at the surface due to a source 4 m above the ground. The zero-offset section is computed for 64 sources, with a hori-


**FIGURE 9**

The retrieved zero-offset result obtained from cross-convolving measured responses at two vertically spaced receivers due to sources in the height level between the two receivers.


**FIGURE 11**

The retrieved zero-offset result obtained from cross-correlating measured responses at two vertically spaced receivers due to sources in the height level above both receivers.


**FIGURE 10**

The retrieved zero-offset result obtained from cross-correlating measured responses at two vertically spaced receivers due to sources in both height levels.

zonal spacing of 10 cm and therefore spans a total horizontal width of just over 6 m. The centre frequency of the source signature is 100 MHz and a temporal sampling of 1 ns is used. In the numerical implementation for the correlation and convolution results we have used 128 sources at different heights and with a horizontal distance of 10 cm between two adjacent sources. At each height interval sources are distributed within a 50 cm vertical band. The first retrieved zero-offset section is obtained by cross-convolving the recordings made at each pair of vertically separated receivers and summing over all sources that are present between the two receiver locations.

The result is shown in Fig. 9, where it can be seen that the actual response is quite accurately retrieved, see e.g. the amplitude behaviour in the neighbourhood of the triplication. Clear spurious events occur in the time window between the direct arrival and the reflections from the syncline structure. These events arise because the contribution from the sources that travel down first and are then recorded at the highest receiver are convolved with the arrival that is directly recorded by the receiver on the surface, which leads to non-physical events. Increasing heterogeneity in the subsurface model will reduce the amplitude of these non-physical events. The second retrieved result is obtained from cross-correlating the received responses at both receivers for each source in the two bands in-between the receivers and above both receivers and summing over all sources.

The result of this process is shown in Fig. 10. Also here the amplitude and arrival times of all physical events are excellent. It can be seen that most non-physical events arrive before the direct wave arrives and presents hardly any problem. It can also be seen that some non-physical events occur in the time window of interest. In the previous section we argued that these events are due to the sources in the lower band that lies between the two receivers. If these sources do not exist the result from only sources that are located at heights above both receivers is shown in Fig. 11. It can be observed that the non-physical events are largely reduced in amplitude and present less of a problem. The reduction of these spurious events has no influence on the amplitudes of the physical events, demonstrating that in the cross-correlation method the presence of sources above all receivers suffices to accurately retrieve the Earth's response between two vertically spaced receivers regardless whether the Earth layers are conductive or not.

## CONCLUSIONS

Using a convenient six-vector notation we have derived several interferometric representations for electromagnetic Green's functions based on reciprocity theorems of the time-convolution and time-correlation types. For practical applications to create data from noise recordings, we found that it is necessary to be able to write these representations in a form that the cross-correlation of two recordings directly leads to the desired Green's function. To allow for such a description it was necessary to rewrite the interaction between electric and magnetic fields in the boundary integral in terms of electric field interactions only, leading to both electric dipole and quadrupole sources in the interferometry results. We have derived relations for the electric field Green's function due to sources of the electric current type and magnetic field Green's functions due to sources of the electric and magnetic current types. All these exact relations require only electric dipole and quadrupole sources on a boundary and both the electric and magnetic field vectors must be recorded. For several scenarios we have demonstrated that it is feasible to find good approximations for the quadrupoles in terms of weighted dipoles and that only electric dipole sources are necessary on the boundary.

Practical acquisition configurations have been suggested for retrieving the Green's matrix of an arbitrarily anisotropic dissipative Earth.

Cross-correlations of electric and magnetic field recordings of present ambient noise, coming from sources in the atmosphere or in space, directly lead to the full electromagnetic Green's function matrix over the bandwidth of the noise power spectrum.

Cross-correlations and cross-convolutions of electric and magnetic field recordings of transient sources, excited well separated in time to allow independent recordings, directly lead to the full electromagnetic Green's function matrix over the bandwidth of the transient sources power spectrum.

Cross-correlations of subsurface electric and magnetic field recordings of ambient noise or transient sources directly yield the Green's function matrix accurately in case the dissipation in the Earth is weak.

## ACKNOWLEDGEMENTS

This research is part of the research programme of The Netherlands Research Center for Solid Earth Science. The authors are grateful to Deyan Draganov for performing the numerical simulations.

## REFERENCES

- Bojarski N. 1983. Generalized reaction principles and reciprocity theorems for the wave equations and the relationships between time-advanced and time-retarded fields. *Journal of the Acoustical Society of America* **74**, 281–285.
- Buckingham M.J., Berkhout B.V. and Glegg S.A.L. 1992. Imaging the ocean with ambient noise. *Nature* **356**, 327–329.
- Cheo B.R.-S. 1965. A reciprocity theorem for electromagnetic fields with general time dependence. *IEEE Transactions on Antennae and Propagation* **13**, 278–284.
- Godin O.A. 2006. Recovering the acoustic Green's function from ambient noise cross correlation in an inhomogeneous moving medium. *Physical Review Letters* **97**, 054301.
- de Hoop A.T. 1995. *Handbook of Radiation and Scattering*. Academic Press.
- Knapp C.H. and Carter G.C. 1976. The generalized correlation method for estimating of time delay. *IEEE Transactions on Acoustics, Speech and Signal Processing* **24**, 320–327.
- Lindell I.V., Sihvola A.H. and Suchy K. 1995. Six-vector formalism in electromagnetics of bi-anisotropic media. *Journal of Electromagnetic Waves Applications* **9**, 887–903.
- Liu L. and He K. 2007. Wave interferometry applied to borehole radar: Virtual multioffset reflection profiling. *IEEE Transactions on Geoscience and Remote Sensing* **45**, 2554–2559.
- Lobkis O.I. and Weaver R.L. 2001. On the emergence of the Green's function in the correlations of a diffuse field. *Journal of the Acoustical Society of America* **110**, 3011–3017.
- Ruf C.S., Swift C.T., Tanner A.B. and Le Vine D.M. 1988. Interferometric synthetic aperture microwave radiometry for the remote sensing of the Earth. *IEEE Transactions on Geoscience and Remote Sensing* **26**, 597–611.
- Scherbaum F. 1987. Seismic imaging of the site response using micro-earthquake recordings: Part I. Method. *Bulletin of the Seismological Society of America* **77**, 1905–1923.
- Schuster G. 2001. Theory of daylight/interferometric imaging: Tutorial. 63<sup>rd</sup> EAGE meeting, Amsterdam, The Netherlands, Expanded Abstracts, A32.
- Schuster G., Yu J., Sheng J. and Rickett J. 2004. Interferometric/daylight seismic imaging. *Geophysical Journal International* **157**, 838–852.
- Slob E., Draganov D. and Wapenaar K. 2006. GPR without a source. *Proceedings of the 11<sup>th</sup> International conference on GPR*, p. ANT.6.
- Slob E., Draganov D. and Wapenaar K. 2007. Interferometric electromagnetic Green's function representations using propagation invariants. *Geophysical Journal International* **169**, 60–80.
- Slob E. and Wapenaar K. 2007a. Electromagnetic Green's functions retrieval by cross-correlation and cross-convolution in media with losses. *Geophysical Research Letters* **34**, L05307.
- Slob E. and Wapenaar K. 2007b. GPR without a source: Cross-correlation and cross-convolution methods. *IEEE Transactions on Geoscience and Remote Sensing* **45**, 2501–2510.
- Snieder R. 2006. Retrieving the Green's function of the diffusion equation from the response to a random forcing. *Physics Review E* **74**, 046620.
- Snieder R. 2007. Extracting the Green's function of attenuating heterogeneous acoustic media from uncorrelated waves. *Journal of the Acoustical Society of America* **121**, 2637–2643.
- Snieder R., Wapenaar K. and Wegler U. 2007. Unified Green's function retrieval by cross-correlation; connection with energy principles. *Physical Review E* **75**, 036103.
- Wapenaar K. 2006. Nonreciprocal Green's function retrieval by cross-correlation. *Journal of the Acoustical Society of America* **120**, EL7–EL13.
- Wapenaar K. 2007. General representations for wave field modeling and inversion in geophysics. *Geophysics* **72**, SM5–SM17.
- Wapenaar K., Draganov D. and Robertsson J. 2008. *Seismic Interferometry: History and Present Status*. SEG (in press).
- Wapenaar K., Fokkema J. and Snieder R. 2005. Retrieving the Green's function in an open system by cross-correlation: A comparison of approaches (L). *Journal of the Acoustical Society of America* **118**, 2783–2786.
- Wapenaar K., Slob E. and Snieder R. 2006. Unified Green's function retrieval by cross-correlation. *Physical Review Letters* **97**, 234301.
- Weaver R.L. and Lobkis O.I. 2001. Ultrasonics without a source: Thermal fluctuation correlations at MHz frequencies. *Physical Review Letters* **87**, 134301.